Preparation and initial characterization of biodegradable particles containing gadolinium-DTPA contrast agent for enhanced MRI

Amber L. Doiron[a], Kevin Chu[a], Adeel Ali[b], and Lisa Brannon-Peppas[c,1]

[a]Department of Biomedical Engineering, University of Texas, Austin, TX 78712; [b]Law Offices of R. V. Reddy, 7171 Harwin Drive, Suite 203, Houston, TX 77036; and [c]Appian Labs, LLC, 11412 Bee Caves Road, Suite 300, Austin, TX 78738

Edited by Robert H. Austin, Princeton University, Princeton, NJ, and approved July 18, 2008 (received for review October 31, 2007)

Accurate imaging of atherosclerosis is a growing necessity for timely treatment of the disease. Magnetic resonance imaging (MRI) is a promising technique for plaque imaging. The goal of this study was to create polymeric particles of a small size with high loading of diethylenetriaminepentaacetic acid gadolinium (III) (Gd-DTPA) and demonstrate their usefulness for MRI. A water-in-oil-in-oil double emulsion solvent evaporation technique was used to encapsulate the MRI agent in a poly(lactide-co-glycolide) (PLGA) or polylactide-poly(ethylene glycol) (PLA-PEG) particle for the purpose of concentrating the agent at an imaging site. PLGA particles with two separate average sizes of 1.83 μm and 920 nm, and PLA-PEG particles with a mean diameter of 952 nm were created. Loading of up to 30 wt % Gd-DTPA was achieved, and *in vitro* release occurred over 5 h. PLGA particles had highly negative zeta potentials, whereas the particles incorporating PEG had zeta potentials closer to neutral. Cytotoxicity of the particles on human umbilical vein endothelial cells (HUVEC) was shown to be minimal. The ability of the polymeric contrast agent formulation to create contrast was similar to that of Gd-DTPA alone. These results demonstrate the possible utility of the contrast agent-loaded polymeric particles for plaque detection with MRI.

atherosclerosis | imaging | targeted | PLGA | PEG

Despite recent advances in medicine and imaging, complications arising from atherosclerosis remain the leading causes of morbidity and mortality in the developed Western world with expectations for growth in coming years (1). Additionally, the financial burden of cardiovascular disease is more than double that of all cancers and is estimated at $430 billion in the United States in direct and indirect costs for 2007 (1). There have been many advances in identifying arterial stenosis, but the most common source of clinical events remains rupturing of vulnerable plaques in vessels with only 50–60% stenosis (2, 3). In fact, only 30–40% of cases of myocardial infarction have a plaque that narrows the artery enough to limit flow (3, 4). Luminal stenosis is delayed until the lesion occupies a significant area within the arterial lamina because of the phenomenon of vascular remodeling (5). The need for stage-specific plaque imaging is paramount because early detection is necessary to predict which patients require aggressive treatment for plaques vulnerable to rupture (6).

The evolution of atherosclerotic plaque is complex and chronic in nature, spanning decades in development from the first microscopic evidence of lipid deposits in the arterial intima to occlusive or thrombus-forming complicated plaques. Atherosclerotic plaques progress through distinct stages with molecular and cellular changes including endothelial dysfunction, the accumulation of oxidized low-density lipoprotein and connective tissue, the involvement of inflammatory and vascular cells, delineation of the plaque into lipid core and fibrous cap regions, and the appearance of fissures or other anomalies (7, 8). Specific stages during the lifespan of the plaque are more vulnerable to rupture because of cellular, molecular, and macroscopic factors including the size and composition of the lipid-rich core, the thickness and integrity of the fibrous cap, active inflammatory responses, and cap fatigue due to chronic repetitive mechanical stresses (7–9). Because of the complex morphological and chemical changes involved in the cascade of atherosclerotic events, imaging of the plaque at a molecular or cellular level is of utmost importance in predicting its likelihood for rupture and identifying the correct treatment.

As a noninvasive imaging modality, magnetic resonance imaging (MRI) is very promising for atherosclerotic plaque imaging because it does not use ionizing radiation, provides high-resolution images of vasculature, is sequentially repeatable, and characterizes the composition of atherosclerotic plaques (10–12). MRI can discriminate plaque constituents such as the lipid core and fibrous cap, plaque burden, and vessel stenosis on the basis of biochemical and biophysical factors (13). Several approaches such as cardiac and respiratory gating, new scan sequences, and the use of contrast agents are being used to improve the spatial resolution and sensitivity limitations of MRI as is necessary for imaging of coronary atherosclerotic plaques.

Drug delivery has long been researched to improve therapeutic efficacy while reducing side effects, and many of the same principles used in this field also augment the delivery of imaging agents to specific physiological locations. Poly(lactide-co-glycolide) is a widely used polymer for these drug delivery systems because it is biodegradable, biocompatible, and widely available, and has been FDA-approved for many biomedical applications (14). Targeted delivery utilizes tissue- or cell-specific phenotypic characteristics to concentrate an active agent at a desired location. Targeted delivery has not only been used for therapeutic purposes but has also recently been researched for its ability to concentrate imaging or contrast agents at a location for the detection of malignancies and for monitoring the effects of therapeutic agents (15).

Gadolinium diethylenetriaminepentaacetic acid is a positive MR contrast agent. This agent has a long history in MR, has been FDA-approved for nearly two decades, and is a well characterized stable chelate. Directly labeling a gadolinium chelate with antibody for targeted delivery has not provided sufficient concentration of agent at the targeted site for *in vivo* imaging, so delivery of a large payload of agent to the site of interest is

This paper results from the Arthur M. Sackler Colloquium of the National Academy of Sciences, "Nanomaterials in Biology and Medicine: Promises and Perils," held April 10–11, 2007, at the National Academy of Sciences in Washington, DC. The complete program and audio files of most presentations are available on the NAS web site at www.nasonline.org/nanoprobes.

Author contributions: A.L.D. and L.B.-P. designed research; A.L.D., K.C., and A.A. performed research; A.L.D., K.C., A.A., and L.B.-P. analyzed data; and A.L.D. and L.B.-P. wrote the paper.

The authors declare no conflict of interest.

This article is a PNAS Direct Submission.

[1]To whom correspondence should be addressed. E-mail: lpeppas@etibio.com.

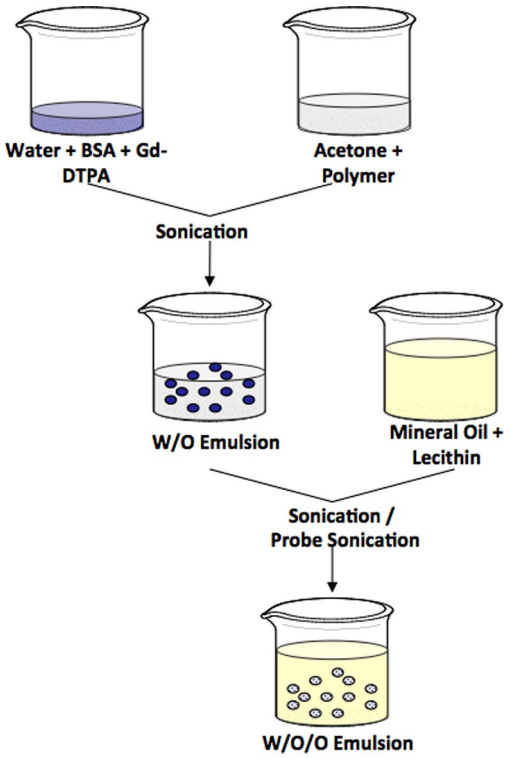

Fig. 1. Schematic of W/O/O protocol showing use of sonication (45 W) or probe sonication (120 W) during formation of second emulsion.

imperative (16, 17). Faranesh and colleagues (18) demonstrated the utility of the inclusion of small amounts of Gd-DTPA in PLGA microparticles for tracking a drug delivery vehicle. Additionally, several groups have created gadolinium-containing micelles, microspheres, nanoparticles, and liposomes for the purposes of targeting delivery or modifying the biodistribution to increase the site-specific concentration of gadolinium over that of aqueous gadolinium or gadolinium directly conjugated to the targeting molecule (19–26). Toward the same goals, this article details a method for the entrapment of hydrophilic agents, specifically Gd-DTPA, with very high loading in a polymeric particulate system as well as work toward achieving a targetable imaging agent particle formulation for the detection of staged atherosclerosis.

Results

Analysis of PLGA Particles. Particles of two different size distributions were synthesized by using a water-in-oil-in-oil (W/O/O) double emulsion method, as schematically shown in Fig. 1, using

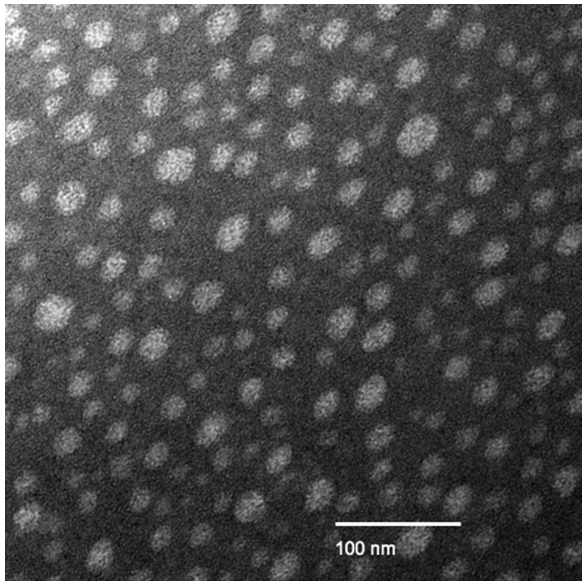

Fig. 3. Transmission electron micrograph of negatively stained PLGA particles prepared by using the W/O/O emulsion with 120-W sonication.

sonication at either 45 or 120 W during the formation of the W/O/O emulsion. The two particle types were characterized separately on the basis of morphology, size, zeta potential, and Gd-DTPA loading. Additionally, the release profile of Gd-DTPA from the particles was determined, and the cytotoxicity of the larger Gd-DTPA-loaded PLGA particles was found by using HUVEC to mimic the arterial endothelium.

Analysis of PLA-PEG Particles. PLA-PEG was polymerized by using the ring opening solution polymerization of lactide onto CM-PEG. The structure of the polymer was confirmed by using ^{1}H-NMR, and the number average molecular weight was found by using gel permeation chromatography (GPC) to be ≈55 kDa with a polydispersity (M_w/M_n) near 1.08, depending on the batch. PLA-PEG nanoparticles were produced by using the W/O/O method with sonication at a 45-W sonic output power, and these particles were evaluated on the basis of morphology, size, zeta potential, and Gd-DTPA encapsulation efficiency and loading.

Particle Characterization. The W/O/O method consistently produced near-spherical particles with smooth surfaces, little agglomeration, and a general size range of 20 nm to 20 μm. Fig. 2 shows the surface characteristics of each particle type as examined by scanning electron microscopy (SEM), and Fig. 3 shows some of the smaller particles as studied with transmission

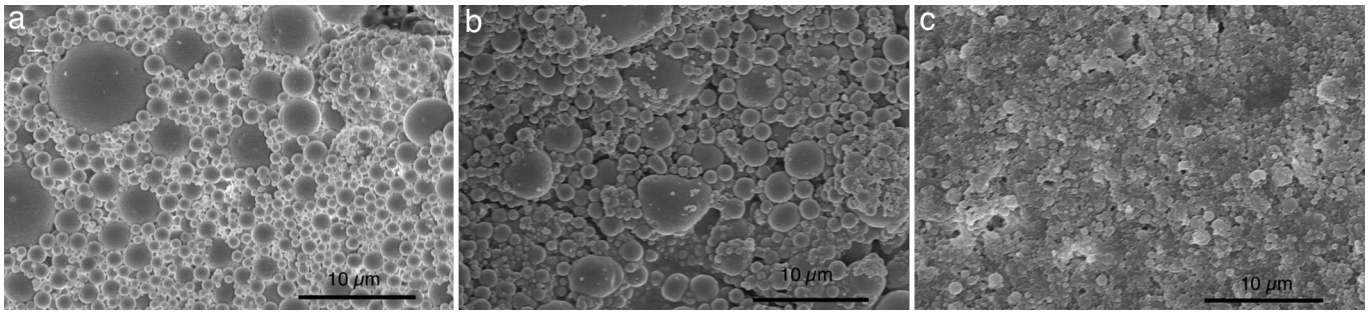

Fig. 2. Scanning electron micrograph of particles containing Gd-DTPA prepared by using the W/O/O emulsion technique. (*a*) PLGA particles prepared by using 45-W sonication for both emulsions. (*b*) PLGA particles prepared by using 120-W sonication during formation of W/O/O emulsion. (*c*) PLA-PEG particles.

Table 1. Particle characteristics

Particle type	Average size	Polydispersity	Zeta potential, mV
PLGA (45-W sonication)	1.83 μm	6 ± 2	−51 ± 8
PLGA (120-W sonication)	920 nm	0.16	−42 ± 6
PLA-PEG (45-W sonication)	952 nm	0.14	−9 ± 3

PLGA (45-W sonication) size was measured by using the Coulter Nanosizer; PLGA (120-W sonication) and PLA-PEG particle sizes were measured with the ZetaPlus instrument.

electron microscopy (TEM). Fig. 2 highlights the differences in particle sizes and size distributions resulting from the different formulation methods. The PLGA particles (Fig. 2 *a* and *b*) all had a rather large size distribution, whereas the PLA-PEG particles (Fig. 2*c*) had a much narrower size distribution.

Zeta Potential and Sizing. Table 1 shows the size ranges and polydispersity indices for each of the three described particle types. The PLGA particles formed by using 45-W sonication for both emulsions were larger than the PLGA particles formed with the probe sonicator at a 120-W output power. The sizes of PLGA particles with the larger mean diameter were measured with a Coulter Nanosizer, whereas the size distributions of the smaller PLGA particles and PLA-PEG particles were measured by using a ZetaPlus instrument. The average zeta potentials of the unloaded PLGA particles differed little with the change in size; however, the PLA-PEG particles had an average zeta potential much closer to neutral. The Tyndall effect was seen for each batch as the particles resuspended well after freeze-drying.

Encapsulation and Loading. Encapsulation and loading as measured by inductively coupled plasma mass spectrometry (ICP-MS) varied depending on the targeted loading of Gd-DTPA, but encapsulation efficiency within PLGA particles (1.83 μm) was typically 30–70% with this method with a maximum Gd-DTPA loading over 50 wt %. The smaller PLGA particles (920 nm) had typical encapsulation efficiencies of 20–50% and loadings up to 25 wt % Gd-DTPA. PLA-PEG particles had encapsulation efficiencies up to 70% and loading up to 15 wt %.

***In Vitro* Release.** The *in vitro* release profile of Gd-DTPA from PLGA particles (1.83 μm) at various loadings in PBS at 37°C is shown in Fig. 4. The release occurred quickly with >90% released in the first hour because of the high hydrophilicity of the entrapped agent. The release was monophasic and occurred over 5 h. The release from smaller PLGA particles (920 nm) follows the same profile and occurs in the same time period, as shown in Fig. 5.

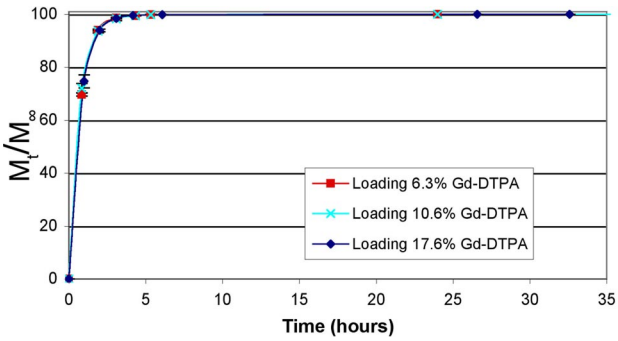

Fig. 4. Release of Gd-DTPA from PLGA particles (1.83 μm) at various loadings. Error bars indicate standard deviation of triplicate samples at a given point.

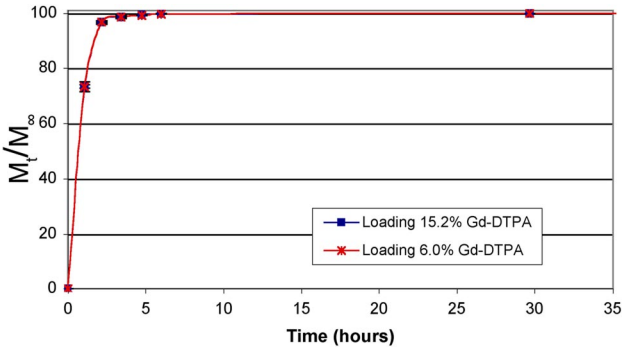

Fig. 5. Release of Gd-DTPA from PLGA particles (920 nm) at various loadings. Error bars indicate standard deviation of triplicate samples at a given time point.

Cytotoxicity. The effects on the viability of human umbilical vein endothelial cells *in vitro* after exposure for 24 h to microparticles (1.83-μm average diameter, targeted loading 20 wt % Gd-DTPA) at concentrations of 10, 20, 50, 100, 200, 500, and 1,000 μg/ml were determined by using an MTS assay, and results are shown in Fig. 6. Additionally, Fig. 7 shows the cumulative effect on HUVEC of tumor necrosis factor α (TNF-α) and PLGA particles (1.83 μm, targeted loading 20 wt % Gd-DTPA) at the same concentrations as above. The microparticles only marginally affected cell viability at high concentrations, and no results were statistically significant from the control as confirmed by ANOVA.

MRI of Particles. The PLGA particles (1.83 μm) loaded with Gd-DTPA effected a change in contrast on MR images as characterized by their longitudinal relaxivity (r_1) as evaluated by using a 1.5-T scanner. Increased loading brought about an increase in r_1 values, but the Gd-DTPA-loaded microparticles had little effect on r_2 values, as was expected at these concentrations. The particle-specific longitudinal relaxivity was found to be 2.37 $ml \cdot s^{-1} \cdot mg^{-1}$ for particles with 54.5% Gd-DTPA loading. The relaxivity of the particle formulation was shown to be similar to that of unencapsulated Gd-DTPA.

Discussion

The PLGA and PLA-PEG particles formulated with the W/O/O method are suitable for encapsulation of Gd-DTPA for the purpose of creating a targetable MR contrast agent for the detection of atherosclerosis. The application of a double emulsion solvent evaporation formulation technique with a hydrophobic oil continuous phase to create small microparticles and nanoparticles to entrap Gd-DTPA has been described. The particles are spherically shaped, stable, and not agglomerated. The encapsulation of Gd-DTPA with this W/O/O protocol is similar to or higher than that shown with other encapsulation methods (18–27). Most importantly, the Gd-DTPA-loaded microparticles were shown to augment contrast in *in vitro* studies similarly to Gd-DTPA alone. The entrapment of Gd-DTPA in a particle allows for the possibility of achieving a high concentration of contrast agent at the imaging site as well as targeting.

Release of Gd-DTPA occurs over a time period appropriate for clinical imaging. The Gd-DTPA is released quickly because of the propensity of the agent to partition into aqueous media. The imaging agent is entrapped within the biodegradable PLGA core and is released through a combination of diffusion through the polymeric matrix and the degradation of the matrix itself. Future projects may aim to contain release more completely during an imaging time period before allowing Gd-DTPA escape from particles. However, a balance must be found between

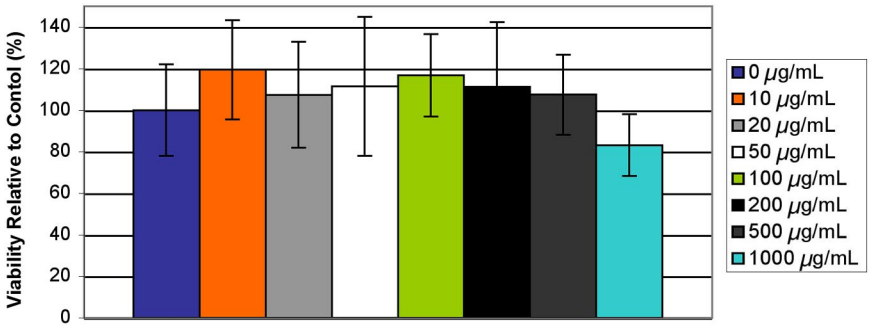

Fig. 6. Viability of HUVEC when exposed to particles (1.83 μm, targeted loading of 20 wt % Gd-DTPA) at concentrations shown in legend as compared to control.

allowing water into the polymer matrix and preventing Gd-DTPA release because the central Gd^{3+} moiety must be hydrated to augment contrast.

Minimal cytotoxic effects were seen even when HUVEC were exposed to high concentrations of particles. This might mimic the situation where targeting concentrates many particles at one local site. The HUVEC line mimics the arterial endothelium during early development of atherosclerosis and was activated in this study by using TNF-α for the purpose of examining the effect of PLGA particles on HUVEC with up-regulated cell-surface receptors such as cell-adhesion molecules.

The size range of particles produced by using the W/O/O protocol can be adjusted depending on the type of sonication used. The use of a probe sonicator has decreased the particle size considerably and reduced the presence of microparticles in the formulations. The two differently sized PLGA particle formulations have been shown here to share similar encapsulation capabilities and release profiles of Gd-DTPA. The advantage of having more than one size distribution is highlighted by the need for a particle that reaches the plaque surface *in vivo*. Particle size has been shown to theoretically affect margination speed and the time needed to reach the vessel wall by circulating particles (28). The complex fluid dynamics in the area of plaque development may necessitate slightly larger particles to overcome being swept away and never entering the boundary layer near the plaque.

As is well known, a particulate formulation has a small likelihood of reaching its desired target before opsonization and recognition by the reticuloendothelial system (RES) unless a method is in place to block this process. Poly(ethylene glycol) (PEG) is widely used to accomplish this goal of reducing opsonization and increasing circulation time from seconds or minutes up to hours (29). This laboratory has investigated the use of a poly(lactic acid)-poly(ethylene glycol) block copolymer with the W/O/O formulation method to synthesize particles with a higher likelihood to bypass the RES. Additionally, the size of theses particles is reduced compared to PLGA particles possibly because of the presence of both hydrophilic and hydrophobic regions in the PLA-PEG polymer. The mean diameter of the PLA-PEG particles was 952 nm with a polydispersity of 0.14. Additionally, zeta potential values closer to neutral than those of PLGA particles reflect changes in surface charge that transpire with the incorporation of PEG.

In addition to the work shown here, this W/O/O method has been used by our laboratory for the encapsulation of other active agents such as Rhodamine 6G. High encapsulation of Rhodamine 6G has been achieved with a slow release occurring over several weeks. This formulation is useful in cellular studies to track particles and their cellular interactions using fluorescence. The possibility for coencapsulation of two imaging agents in these particles exists and is attractive for the study of the particles by using more than one imaging modality.

Materials and Methods

Synthesis of PLGA Particles. Particles were synthesized by using a water-in-oil-in-oil (W/O/O) double emulsion solvent evaporation method based on a procedure described by Chaw and colleagues (30). Several steps in the protocol were optimized for particle morphology and size as well as entrapment of the active agent Gd-DTPA (data not shown). These optimized factors included emulsifier concentration, type of mechanical agitation (sonication, vortexing, stirring, etc.), centrifugation speed and time, and inclusion of cryoprotectant during freezing and freeze-drying to arrive at this final protocol. The PLGA polymer (Medisorb; M_n = 11 kDa) was dissolved at a concentration of 80 mg/ml in 1.25 ml of acetone (HPLC grade; Fisher Scientific) to form the polymer phase. Diethylenetriaminepentaacetic acid gadolinium (III) dihydrogen salt hydrate (Sigma) was dissolved in an aqueous solution of BSA (10 mg/ml; Sigma) at a concentration of 0–50 mg/ml. The external oil phase was comprised of egg lecithin (Acros) at a concentration of 0.0625 mg/ml in light mineral oil (Sigma). The aqueous phase (500 μl) was added to the polymer phase and sonicated at an average sonic power of 45 W (VWR Model 50D). This primary W/O emulsion was subsequently added to the external oil phase (25 ml) and either sonicated with a bench-top sonicator at 45 W for 1 min

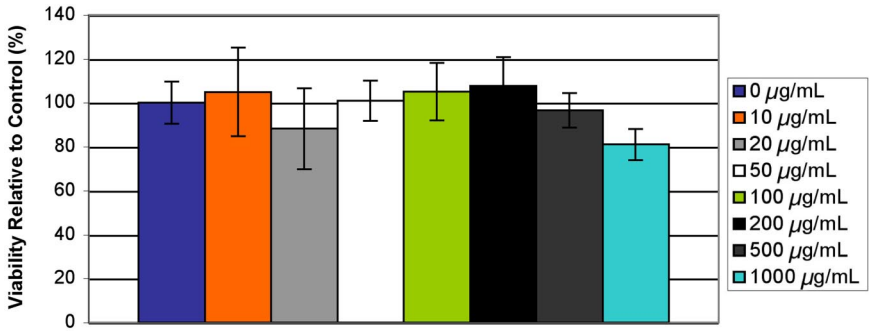

Fig. 7. Viability of HUVEC activated by TNF-α when exposed to particles (1.83 μm, targeted loading of 20 wt % Gd-DTPA) at concentrations shown in legend as compared to control.

to create the larger average size particles or for 10 min with a Misonix XL2020 probe sonicator at an output power of 120 W to create the smaller sized particles. The solution was stirred at 500 rpm during vacuum evaporation for 45 min to remove organic solvent. Particles were collected with centrifugation at 43,000 × *g* for 15 min at 4°C and washed three times with hexane (HPLC grade; Acros) to remove mineral oil. Hexane was removed, and the particles were frozen for 12–24 h and freeze-dried (Labconco Freeze Dryer 4.5) for a period of 48 h. Particles were stored at −20°C until further analysis.

Synthesis of PLA-PEG Particles. Poly(lactic acid)-poly(ethylene glycol) block copolymer was prepared for use with the W/O/O particle formulation method. The PLA-PEG copolymer was prepared by ring opening polymerization of lactide in the presence of carboxymethyl-poly(ethylene glycol) (CM-PEG), using a procedure modified from Quellec and colleagues (31). Briefly, recrystallized DL-lactide monomer (Polysciences) was polymerized onto CM-PEG (molecular weight 3,400; Laysan Bio) in the presence of stannous 2-ethylhexanoate (Sigma) in toluene (anhydrous; Acros) at 110°C under a nitrogen atmosphere. The product was recovered by centrifugation after dissolution in methylene chloride (Fisher Scientific) and precipitation in ethyl ether (anhydrous; Fisher Scientific). The polymer product was confirmed by ^{1}H-NMR, and the molecular weight was quantified by using GPC. The PLA-PEG was then used to synthesize particles by the W/O/O method in the same manner described above, using the bench-top sonicator for both sonication steps. The addition of trehalose as a cryoprotectant during freezing and freeze drying aided in stabilizing particles against agglomeration, as suggested by other investigators (32, 33).

Particle Characterization. Particles were analyzed by using SEM for morphology and size. Particles were evaluated on the basis of shape, surface smoothness, and the presence of agglomeration or interparticular bridging. Additionally, the size range was judged qualitatively by SEM. Particle samples for SEM were prepared by suspending a small amount of the lyophilized particles in deionized water and allowing the suspension to dry on conductive tape on top of a metallic stud before sputter coating with gold. Images were captured at a 10-kV accelerating voltage on a Hitachi S-4500 field emission SEM. A Phillips EM 208 transmission electron microscope (TEM) was used to confirm particle size and to study samples at high magnification. Particles were suspended in deionized water, dried on a 300 mesh copper TEM grid with a carbon film (Electron Microscopy Sciences), and stained with uranyl acetate (Baker Chemical).

Zeta Potential and Sizing. Zeta-potential measurements were taken to verify the stability of the colloid suspension. Gd-DTPA interfered with zeta-potential measurements as it increased the conductance of the solution, so tests were run with particles formulated by the W/O/O method in the absence of Gd-DTPA. Lyophilized particles were suspended at 1 mg/ml by sonication in a 1 mM KCl electrolyte solution, and the zeta potential and size were measured at 25°C with a ZetaPlus instrument with accompanying software (Brookhaven Instruments). The instrument used electrophoretic light scattering and the laser Doppler velocimetry method to measure the zeta potential and number average distribution of particle sizes. The size distributions of the PLGA particles formulated by using the probe sonicator and the PLA-PEG particles were measured by using the ZetaPlus, and the polydispersity was given as a reading from 0 to 1. The size of PLGA particles formulated by using the bench-top sonicator for both sonication steps was measured with a Coulter Nanosizer dynamic light scattering instrument with the polydispersity given as an index from 0 to 9. As mentioned above, the size was also qualitatively verified by using SEM, and all measurements were done on previously lyophilized samples.

Encapsulation and Loading. Active agent loading and encapsulation efficiency were determined by quantifying the amount of Gd in a representative sample of each Gd-DTPA particle batch by ICP-MS, using an OptiMass 8000 spectrometer with OptiMass software (version 1.2; GBC Scientific Equipment). The correct isotopic ratios were confirmed, and the absence of interference by the polymer was verified. A known mass of particles was suspended in deionized distilled water by sonication, and volumetric dilutions were done to achieve an approximate Gd concentration within the detection limits of the spectrometer. Counts of Gd were correlated to a concentration of Gd-DTPA based on a standard curve generated by using Gd-DTPA.

***In Vitro* Release.** A known mass of lyophilized particles was suspended in 20 ml of PBS (Sigma) at pH 7.4 and left in a 37°C waterbath for a specified period. Samples were centrifuged at 43,000 × *g* for 15 min at 20°C, and 75% of the supernatant was collected and replaced with fresh PBS. Supernatant samples were analyzed by ICP-MS as described above. This procedure was repeated until no additional release was detected, and the remaining pellet was analyzed for unreleased Gd-DTPA. Release assessed by this static test did not to differ significantly from release occurring with sample agitation, and thus the static test was used because of simplicity.

Cytotoxicity. The cytotoxicity of the Gd-DTPA-loaded PLGA particles was determined by using a colorimetric 3-(4,5-dimethyl-2-yl)-5-(3-carboxymethoxyphenyl)-2-(4-sulfophenyl)-2H-tetrazolium (MTS) assay based on the conversion of the tetrazolium salt into a formazan product by viable cells. The characteristic absorbance of the formazan product was used to determine the percentage of viable cells when compared to control cells grown without exposure to particles. TNF-α (Sigma) was used to up-regulate cell-adhesion molecules on HUVEC to be used later for a simple *in vitro* targeting scheme. Pooled HUVEC (Lonza/Clonetics) were cultured for 24 h in endothelial growth medium (EGM) (Lonza/Clonetics) at 37°C with 5% CO_2 in a 96-well plate after splitting from T-25s at second passage (2,000 cells per well). Plate wells and flasks were coated with 0.1% gelatin (Difco/Becton Dickinson) in Dulbecco's PBS (Mediatech) 3 h before plating with cells. Cells were exposed to Gd-DTPA-loaded PLGA particles (targeted loading 20 wt % Gd-DTPA, 45-W sonication) for 24 h and 0 or 10 ng/ml TNF-α for 8 h. Promega CellTiter 96 AQueous One Solution Cell Proliferation Assay was added to the wells and allowed to incubate for 4 h. The absorbance was measured at 490 nm and at a reference wavelength of 700 nm to assess viability of cells in the presence of PLGA particles compared to cells not exposed to particles. A one-way ANOVA was run to examine statistical differences in absorbance after verifying that the data followed a normal distribution.

MRI of Particles. *In vitro* r_1 and r_2 relaxivities were determined for Gd-DTPA-loaded PLGA particles and unloaded PLGA particles suspended at 1 mg/ml in agarose gels (1.5 wt % agarose prepared with deionized water), using a 1.5-T scanner (Excite HD; GE Healthcare) accompanied by a GE Quad Ankle coil. Suspended particles containing Gd-DTPA from 0 to 0.5 mM were scanned and compared to the same concentrations of unencapsulated Gd-DTPA. For T_1 measurements, an inversion recovery (2D IR) sequence was used with the following imaging parameters: TR = 3,000 ms; TE = 14 ms; TI = 50, 70, 100, 200, 250, 300, 400, 500, 600, 700, 800, 900, 1,000, 2,000, 2,950 ms; band width of 15.6 kHz; FOV of 18 × 9 cm; slice thickness of 4.0 mm; matrix of 256 × 128; and a flip angle of 90°. For the T_2 measurements, a 2D SE sequence was used with a TR = 4,000 ms; TE = 16, 20, 30, 40, 60, 80, 100, 200, 300 ms; band width of 15.6 kHz; FOV of 18 × 9 cm; slice thickness of 4.0 mm; matrix of 256 × 128; and flip angle of 90°. Values for r_1 and r_2 were determined where r_1 and r_2 are the inverse of T_1 and T_2, respectively.

ACKNOWLEDGMENTS. We thank John Hazle, Ph.D., and Andrew Elliot, Ph.D., for their help with magnetic resonance imaging at M. D. Anderson Cancer Center, as well as James Holcolmbe, Ph.D., Thomas Kreschollek, Ph.D., and Haley Finley-Jones for the ICP-MS work. This work was supported by the American Heart Association and the National Science Foundation Integrative Graduate Education and Research Traineeship (IGERT) program.

1. Rosamond W, *et al.*, for the American Heart Association Statistics Committee and Stroke Statistics Subcommittee (2007) Heart disease and stroke statistics—2007 update—A report from the American Heart Association Statistics Committee and Stroke Statistics Subcommittee. *Circulation* 115:e69–e171.
2. Brown BG, *et al.* (1986) Incomplete lysis of thrombus in the moderate underlying atherosclerotic lesion during intracoronary infusion of streptokinase for acute myocardial infarction: Quantitative angiographic observations. *Circulation* 73:653–661.
3. Ambrose JA, *et al.* (1988) Angiographic progression of coronary-artery disease and the development of myocardial-infarction. *J Am Coll Cardiol* 12:56–62.
4. Little WC, *et al.* (1988) Can coronary angiography predict the site of a subsequent myocardial-infarction in patients with mild-to-moderate coronary-artery disease. *Circulation* 78:1157–1166.
5. Glagov S, Weisenberg E, Zarins CK (1987) Compensatory enlargement of human atherosclerotic coronary-arteries. *N Engl J Med* 316:1371–1375.
6. Rudd JHF, Davies JR, Weissberg PL (2005) Imaging of atherosclerosis—Can we predict plaque rupture? *Trends Cardiovasc Med* 15:17–24.
7. Stary HC, *et al.* (1994) A definition of initial, fatty streak, and intermediate lesions of atherosclerosis—A report from the Committee on Vascular Lesions of the Council on Arteriosclerosis, American Heart Association. *Circulation* 89:2462–2478.
8. Stary HC, *et al.* (1995) A definition of advanced types of atherosclerotic lesions and a histological classification of atherosclerosis—A report from the Committee on Vascular Lesions of the Council on Arteriosclerosis, American Heart Association. *Circulation* 92:1355–1374.
9. Dalager-Pedersen S, Pedersen EM, Ringgaard S, Falk E (1999) in *The Vulnerable Atherosclerotic Plaque: Understanding, Identification, and Modification*, ed Fuster V (Blackwell, New York), pp 1–23.
10. Choudhury RP, Fuster V, Fayad ZA (2004) Molecular, cellular and functional imaging of atherothrombosis. *Nat Rev Drug Discovery* 3:913–925.

11. Cai JM, *et al.* (2002) Classification of human carotid atherosclerotic lesions with in vivo multicontrast magnetic resonance imaging. *Circulation* 106:1368–1373.
12. Luk-Pat GT, Gold GE, Olcott EW, Hu BS, Nishimura DG (1999) High-resolution three-dimensional in vivo imaging of atherosclerotic plaque. *Magn Reson Med* 42:762–771.
13. Fayad ZA, Fuster V (2001) Clinical imaging of the high-risk or vulnerable atherosclerotic plaque. *Circ Res* 89:305–316.
14. Jain RA (2000) The manufacturing techniques of various drug loaded biodegradable poly(lactide-co-glycolide) (PLGA) devices. *Biomaterials* 21:2475–2490.
15. Brannon-Peppas L, Blanchette JO (2004) Nanoparticle and targeted systems for cancer therapy. *Adv Drug Delivery Rev* 56:1649–1659.
16. Funovics MA, *et al.* (2004) MR imaging of the her2/neu and 9.2.27 tumor antigens using immunospecific contrast agents. *Magn Reson Imaging* 22:843–850.
17. Gohr-Rosenthal S, Schmitt-Willich H, Ebert W, Conrad J (1993) The demonstration of human tumors on nude mice using gadolinium-labeled monoclonal-antibodies for magnetic resonance imaging. *Invest Radiol* 28:789–795.
18. Faranesh AZ, *et al.* (2004) In vitro release of vascular endothelial growth factor from gadolinium-doped biodegradable microspheres. *Magn Reson Med* 51:1265–1271.
19. Lipinski MJ, *et al.* (2006) MRI to detect atherosclerosis with gadolinium-containing immunomicelles targeting the macrophage scavenger receptor. *Magn Reson Med* 56:601–610.
20. Ayyagari AL, *et al.* (2006) Long-circulating liposomal contrast agents for magnetic resonance imaging. *Magn Reson Med* 55:1023–1029.
21. Robertson JD, Crane SB, Wickline SA, Lanza GM (2005) Characterization and biodistribution of a novel MRI molecular imaging agent by neutron activation analysis. *J Radioanal Nucl Chem* 263:511–514.
22. Winter PM, *et al.* (2003) Molecular imaging of angiogenesis in early-stage atherosclerosis with $\alpha(v)\beta(3)$-integrin-targeted nanoparticles. *Circulation* 108:2270–2274.
23. Flacke S, *et al.* (2001) Novel MRI contrast agent for molecular imaging of fibrin: Implications for detecting vulnerable plaques. *Circulation* 104:1280–1285.
24. Reynolds CH, *et al.* (2000) Gadolinium-loaded nanoparticles: New contrast agents for magnetic resonance imaging. *J Am Chem Soc* 122:8940–8945.
25. Chen HH, *et al.* (2005) MR imaging of biodegradable polymeric microparticles: A potential method of monitoring local drug delivery. *Magn Reson Med* 53:614–620.
26. Amirbekian V, *et al.* (2007) Detecting and assessing macrophages in vivo to evaluate atherosclerosis noninvasively using molecular MRI. *Proc Natl Acad Sci USA* 104:961–966.
27. Tokumitsu H, Ichikawa H, Fukumori Y (1999) Chitosan-gadopentetic acid complex nanoparticles for gadolinium neutron-capture therapy of cancer: Preparation by novel emulsion-droplet coalescence technique and characterization. *Pharm Res* 16:1830–1835.
28. Decuzzi P, Lee S, Bhushan B, Ferrari M (2005) A theoretical model for the margination of particles within blood vessels. *Ann Biomed Eng* 33:179–190.
29. Owens DE, Peppas NA (2006) Opsonization, biodistribution, and pharmacokinetics of polymeric nanoparticles. *Int J Pharm* 307:93–102.
30. Chaw CS, Yang YY, Lim IJ, Phan TT (2003) Water-soluble β-methasone-loaded poly-(lactide-co-glycolide) hollow microparticles as a sustained release dosage form. *J Microencapsulation* 20:349–359.
31. Quellec P, *et al.* (1998) Protein encapsulation within polyethylene glycol-coated nanospheres I. Physicochemical characterization. *J Biomed Mater Res* 42:45–54.
32. De Jaeghere F, *et al.* (1999) Formulation and lyoprotection of poly(lactic acid-co-ethylene oxide) nanoparticles: Influence on physical stability and in vitro cell uptake. *Pharm Res* 16:859–866.
33. Chacon M, Molpeceres J, Berges L, Guzman M, Aberturas MR (1999) Stability and freeze-drying of cyclosporine loaded poly(D,L-lactide-glycolide) carriers. *Eur J Pharm Sci* 8:99–107.